

Infrared Imaging of the Gravitational Lens PG 1115+080 with the Subaru Telescope

Fumihide IWAMURO,¹ Kentaro MOTOHARA,¹ Toshinori MAIHARA,¹ Jun'ichi IWAI,¹
 Hirohisa TANABE,¹ Tomoyuki TAGUCHI,¹ Ryuji HATA,¹ Hiroshi TERADA,¹ Miwa GOTO,¹
 Shin OYA,⁵ Masayuki AKIYAMA,^{2,3} Hiroyasu ANDO,⁴ Tetsuo AOKI,⁵ Yoshihiro CHIKADA,³
 Mamoru DOI,⁶ Takeo FUKUDA,⁷ Masaru HAMABE,⁸ Masahiko HAYASHI,² Saeko HAYASHI,²
 Toshihiro HORAGUCHI,⁹ Shinichi ICHIKAWA,¹⁰ Takashi ICHIKAWA,¹¹ Masatoshi IMANISHI,⁴
 Katsumi IMI,² Motoko INATA,⁴ Shuzo ISOBE,⁴ Yoichi ITOH,² Masanori IYE,⁴ Norio KAIFU,²
 Yukiko KAMATA,⁷ Tomio KANZAWA,² Hiroshi KAROJI,⁴ Nobunari KASHIKAWA,⁴ Taichi KATO,³
 Naoto KOBAYASHI,² Yukiyasu KOBAYASHI,⁴ Keiichi KODAIRA,¹² George KOSUGI,²
 Tomio KURAKAMI,² Yoshitaka MIKAMI,⁴ Akihiko MIYASHITA,² Takashi MIYATA,⁴
 Satoshi MIYAZAKI,⁷ Yoshihiko MIZUMOTO,⁴ Masao NAKAGIRI,⁴ Koich NAKAJIMA,¹³
 Kyoko NAKAMURA,⁷ Kyoji NARIAI,¹² Eiji NISHIHARA,¹⁰ Jun NISHIKAWA,⁴ Shiro NISHIMURA,¹²
 Tetsuo NISHIMURA,² Tetsuo NISHINO,⁷ Kunio NOGUCHI,⁴
 Takeshi NOGUCHI,⁴ Jun'ichi NOUMARU,² Ryusuke OGASAWARA,² Norio OKADA,⁷
 Kiichi OKITA,⁴ Koji OMATA,² Norio OSHIMA,⁷ Masashi OTSUBO,² Goro SASAKI,⁷
 Toshiyuki SASAKI,² Maki SEKIGUCHI,¹⁴ Kazuhiro SEKIGUCHI,² Ian SHELTON,² Chris SIMPSON,²
 Hiroshi SUTO,¹ Hideki TAKAMI,⁴ Tadafumi TAKATA,² Naruhisa TAKATO,⁴ Motohide TAMURA,⁴
 Kyoko TANAKA,⁴ Wataru TANAKA,⁴ Daigo TOMONO,² Yasuo TORII,⁴ Tomonori USUDA,²
 Koichi WASEDA,⁷ Jun'ichi WATANABE,¹⁵ Masaru WATANABE,¹⁰ Masafumi YAGI,⁴
 Takuya YAMASHITA,² Yasumasa YAMASHITA,¹² Naoki YASUDA,⁴ Michitoshi YOSHIDA,⁴
 Shigeomi YOSHIDA,¹⁶ and Masami YUTANI,⁴

¹*Department of Physics, Kyoto University, Kitashirakawa, Kyoto 606-8502*

E-mail(FI): iwamuro@cr.scphys.kyoto-u.ac.jp

²*Subaru Telescope, National Astronomical Observatory, 650 North Aohoku Place, Hilo, HI 96720, USA*

³*Department of Astronomy, Kyoto University, Kyoto 606-8502*

⁴*Optical and Infrared Astronomy Division, National Astronomical Observatory, Mitaka, Tokyo 181-8588*

⁵*Communications Research Laboratory, Koganei, Tokyo 184-8975*

⁶*Department of Astronomy, The University of Tokyo, Bunkyo-ku, Tokyo 113-0033*

⁷*Advanced Technology Center, National Astronomical Observatory, Mitaka, Tokyo 181-8588*

⁸*Institute of Astronomy, The University of Tokyo, Mitaka, Tokyo 181-8588*

⁹*National Science Museum, Taito-ku, Tokyo 110-8718*

¹⁰*Astronomical Data Analysis Center, National Astronomical Observatory, Mitaka, Tokyo 181-8588*

¹¹*Astronomical Institute, Tohoku University, Aoba-ku, Sendai 980-8578*

¹²*National Astronomical Observatory, Mitaka, Tokyo 181-8588*

¹³*Hitotsubashi University, Kunitachi, Tokyo 186-8601*

¹⁴*Cosmic Ray Research Laboratory, The University of Tokyo, Tanashi, Tokyo 188-8502*

¹⁵*Public Relation Office, National Astronomical Observatory, Mitaka, Tokyo 181-8588*

¹⁶*Kiso Observatory, The University of Tokyo, Mitake, Nagano 397-0101*

(Received 1999 May 18; accepted 1999 August 6)

Abstract

We present high spatial resolution images of the gravitational-lens system PG 1115+080 taken with the near-infrared camera (CISCO) on the Subaru telescope. The FWHM of the combined image is $0''.32$ in the K' -band, yielding spatial resolution of $0''.14$ after a deconvolution procedure. This is a first detection of an extended emission adjacent to the A1/A2 components, indicating the presence of a fairly bright emission region with a characteristic angular radius of ~ 5 mas (40 pc). The near-infrared image of the Einstein ring was extracted in both the J and K' bands. The $J - K'$ color is found to be significantly redder than that of a synthetic model galaxy with an age of 3 Gyr, the age of the universe at the quasar redshift.

Key words: galaxies: structure — gravitational lensing — quasars: individual (PG 1115+080)

1. Introduction

The quadruply imaged $z = 1.722$ quasar PG 1115+080 (Weymann et al. 1980) is one of the gravitational lens systems in which time delays have been measured (Schechter et al. 1997; Barkana 1997). Astrometric and photometric observations have been made by HST (Kristian et al. 1993; Impey et al. 1998) and by ground-based telescopes (Courbin et al. 1997). As a result, they have precisely determined the radial offset of each lensed component from the lensing galaxy, which is located at a redshift of 0.311 (Kundic et al. 1997; Tonry 1998). Restrictions on the Hubble constant were obtained on the basis of these observational materials along with appropriate lens models (Courbin et al. 1997; Kundic et al. 1997; Keeton, Kochanek 1997; Saha, Williams 1997; Impey et al. 1998).

A gravitational-lens system also offers an opportunity to study the detailed structure of the lensed object, because the lens effect serves as a *natural telescope* which magnifies and brightens the image of the lensed object, although the lensed images are distorted.

Recently, the infrared Einstein ring of PG 1115+080 was found (Impey et al. 1998) using the NICMOS camera, which is supposed to represent emission from the quasar host galaxy.

In this letter, we report on the results of near-infrared observations of PG 1115+080 made with the 8.2 m Subaru telescope, which was installed on the summit of Mauna Kea, Hawaii, at the end of 1998. Even in the very first stage of observations in early 1999 January, nearly ultimate performance as a ground-based, large mirror telescope has been demonstrated, as discussed in the following.

Based on J and K' band images taken under an $\sim 0''.3$ seeing condition, we present the detection of the Einstein ring in both bands, the distortion of the A1/A2 profiles in the deconvolved image, and the structure of the quasar host galaxy.

2. Observations and Data Reduction

Photometric observations of PG 1115+080 were made on 1999 Jan 11 and 13 using the near-infrared camera CISCO (Motohara et al. 1998) mounted on the Cassegrain port of the 8.2 m Subaru Telescope on Mauna Kea. The camera uses a 1024×1024 element HgCdTe array (HAWAII; Kozlowski et al. 1994; Hodapp et al. 1996) with a pixel scale of $0''.116 \text{ pixel}^{-1}$, giving a total field of view of $2' \times 2'$. Although the exposure time for the normal full-frame readout is usually no shorter than 1.5 s/frame, in the present observations we utilized a fast-readout mode, by which subarray regions (64×64 or 128×128 pixels in the corner of each quadrant) could be sampled faster, with the minimum being 0.025 s/frame.

Fortunately, there is, by chance, a reference star (star A in figure 1) located in one of the 128×128 subarray regions while aiming at PG 1115+080 in the other quadrant, so that both objects could be observed simultaneously.

For the cancelation of sky emission we periodically moved the telescope in the north-south direction, by $6''$ after taking 96 frames at one position with an exposure time of 0.3 s/frame. The total numbers of frames obtained were 3456 and 4032 in the J - and K' -band, respectively, giving overall integration times of 1037 s (J) and 1210 s (K').

The obtained data were reduced through standard common processes of sky subtraction, flat-fielding, and the correction of bad pixels. After each pixel was divided into 4×4 sub-pixels, the images were shifted and added by reference to the center of gravity of the stellar image of star A. Since we noticed that the point-spread function (PSF) profiles are not exactly the same between the object position and the position of star A, possibly due to the nature of the optical system of CISCO, the PSF of star A was linearly transformed using the matrix with values of elements in table 1,

$$\begin{pmatrix} \cos \theta & -\sin \theta \\ \sin \theta & \cos \theta \end{pmatrix} \begin{pmatrix} a & 0 \\ 0 & b \end{pmatrix} \begin{pmatrix} \cos \theta & \sin \theta \\ -\sin \theta & \cos \theta \end{pmatrix} \quad (1)$$

so as to make component C of PG 1115+080 to be a virtual point source. Finally, PSF subtraction and MEM deconvolution were applied to the combined image using this transformed PSF.

3. Results

Analyses of the PSF of the recorded images in the J - and K' -bands were performed using the IRAF image processing package, providing histograms of the statistical distribution of the FWHM values, as presented in figure 2. The images with FWHMs larger than $0''.45$ ($\sim 20\%$ out of the frames recorded) were excluded in the shift and add procedure so as to secure better images, which are displayed in figures 3a and b. The resultant co-added images of star A are represented by FWHMs of $0''.36$ and $0''.32$ in the J - and K' -bands, respectively (figures 4a and b). The photometry of each component was carried out within a circular aperture of $0''.86$ diameter. In reducing calibrated fluxes of individual sources, flux corrections were applied by adding the relative contribution in the outskirts region of the transformed PSF, which would, otherwise, be excluded by the $0''.86$ aperture photometry. The result is presented in table 2.

As for the spatial structure of the lensing galaxy, it is assumed that the intrinsic radial distribution of the sur-

face brightness has a de Vaucouleurs profile (figures 4c and d), and that the parameters describing the galaxy have been determined. The actual method is, first, to convolve the de Vaucouleurs expression with appropriate parameters using the transformed PSF, and then to compare it with the observed profile. The results are an effective radius R_e of $0''.58 \pm 0''.05$, the surface brightness in the center, $\mu_e = 19.74/17.90 \pm 0.05$ mag arcsec $^{-2}$ (in the J/K' band), the ellipticity, $\varepsilon \approx 0.1$, and a position angle θ of $\sim 65^\circ$.

The photometric error of the zero point is estimated to be ~ 0.05 mag, which is mostly attributed to the uncertainty in the photometry of star A, whose magnitudes were determined by measuring faint standard stars, such as FS 19 and FS 21 of the UKIRT FS Catalog (Casali, Hawarden 1992), with identical observing configurations. The $J - K'$ colors of the respective components in the image are also given in table 2.

It should be noted that component A1 is significantly bluer than other split-image components, which may be associated with the fact that the fairly large flux ratio in the A1/A2 pair can not be interpreted using a normal simple lensing configuration.

A somewhat asymmetric annulus of the Einstein ring is shown to remain when subtracting all of the lensed components A1, A2, B, and C and the lensing galaxy G in both the J and K' bands. In presenting the surface brightness of the ring, we select two particular regions (R1 and R2 in figure 3e and f) where the brightness of the Einstein ring suffers less from the uncertainty caused by the process of removing the images of the A1/A2 system. The results are given in the lower lines of table 2. A two-color image produced from figures 3e and f is shown in figure 5a. The implication of this reddish color is discussed later.

With the MEM deconvolution task in the IRAF STSDAS package, we deconvolved images of the two bands so as to produce a high spatial resolution color image of the quasar, as presented in figure 5b, where the source size is $0''.14$ in FWHM. It is important to note that the B and C components are simply round shaped, while the A1/A2 system is significantly different from a symmetric shape. The meaning of this elongated morphology is briefly interpreted in the following discussion.

4. Discussion

The spectral energy distributions (SEDs) of the components of the PG 1115+080, including the Einstein ring, are plotted in figure 6, where the data presented in past literature are added (see inset captions). The quasar spectrum appears to be flat (the index of power being nearly zero) over the observed wavelength range, except for the blue bump at around the 250 nm region. The

flat nature of SEDs with a distinctive blue bump is typical of quasars with a pole-on geometry (Baker, Hunstead 1995; Baker 1997). The absorption-free spectrum indicates that the central source is obscured neither by the host galaxy nor by the intervening lensing galaxy.

On the contrary, the ring regions show considerable red colors, even after allowing for the uncertainties, as indicated by the error bars in the figure. In the meantime, from a model calculation of the gravitational lens system, which is basically the same method described as that by Keeton et al. (1998), it is seen that the regions designated by R1 and R2 lie at galactocentric distances of ~ 2 kpc and ~ 1 kpc, respectively. By comparing the SEDs of synthetic model galaxies based on those of nearby galaxies of various types, we can see that two-band photometry data of the host galaxy appear to correspond to that of an aged galaxy older than 3 Gyr, or even to E/S0 galaxies. Here, we refer to the SEDs presented by Coleman et al. (1980) for nearby galaxies; the modeled SED was calculated using the code given by Floc and Rocca-Volmerange (1997), in which we adopted an exponential burst star-formation model with a time scale of $\tau_0 = 1$ Gyr.

It is interesting to note that an inferred age of 3 Gyr corresponds to the age of the universe at the quasar redshift. Here, we take $H_0 = 75$ km s $^{-1}$ Mpc $^{-1}$ and $q_0 = 0.1$ for cosmological parameters.

The present result deduced from the unexpectedly red color of the host galaxy could be interpreted either by 1) a hypothesis that the host galaxy contains a certain amount of dust, thus making the color appreciably redder than nearby starburst galaxies, or 2) the case that the color is intrinsically red with negligible internal absorption.

In the latter case, however, an age of >3 Gyr of the galaxy contradicts an epoch of $z = 1.72$ of the Universe. Virtually instantaneous star formation with a particular initial mass function (IMF) could ease the situation, because the contribution of asymptotic giant branch (AGB) stars in the mass range from 5 to $10 M_\odot$ makes an SED fairly red on a time scale of ~ 1 Gyr. As for the former case, the dusty environment in the host galaxy is not necessarily unrealistic, although the quasar light apparently suffers from no significant dust extinction, because the dust in the line of sight could be blown off by the intermittent jet activities reported by Michalitsianos et al. (1996). To clarify the nature of the overall spectrum of the host galaxy, further detailed spectroscopic observations are required.

The observed fluxes at J and K' of the lensing galaxy are plotted in accord with a typical SED of the E/S0 galaxy (Coleman et al. 1980; Yoshii & Takahara 1988). It has also been confirmed that the obtained radial distribution of the surface brightness is well represented by the de Vaucouleurs profile and, moreover, that the shape is slightly, but significantly, ellipsoidal, as found by Im-

pey et al. (1998). The fitted position angle of the ellipsoid is $\theta \approx 65^\circ$, consistent with the result of Keeton et al. (1998) in which they report that the position angles of the optical axis of ellipsoids generally agree with those of the modeled mass distribution in most cases of gravitational-lens systems. In particular, they predicted a position angle of PG 1115+0080 as being 67° , which is the same as the light distribution given by the present observation.

Finally, let us remark that the image profiles of the quasar, exhibit a deformed shape of the A1 and A2 components (see figure 5). These elongated emission components, whose color is quite similar to that of the quasar, itself, is believed to be real in view of the observational accuracy. In a quantitative analysis using the model calculation of the present lens system, we found that the circumnuclear emission as close as ~ 40 pc (~ 5 mas) to the central quasar should be responsible for the bridge-like structure connecting components A1 and A2. Because the radial distance is considerably larger than the size of the typical broad line region (<1 pc), we speculate that the light originates from illumination caused by electron scattering, supposedly taking place near to the surface of the surrounding toric gaseous cloud, from where electrons are supplied by intense ionizing radiation of the central source. In this view, the exact line of sight to the quasar is presumed to be virtually free from absorbing or scattering material; such a configuration is consistent with the observed quasar spectrum, as formerly pointed out.

The present result, accomplished as one of the first-light observing programs of the Subaru Telescope, is indebted to all members of Subaru Observatory, NAOJ, Japan. We would like to express thanks to the engineering staff of Mitsubishi Electric Co. for the fine operation of the telescope, and the staff of Fujitsu Co. for timely provision of control software. The authors are grateful to M. Fioc and B. Rocca-Volmerange for the generous offer to provide their galaxy-modeling code, PEGASE.

References

- Baker J.C. 1997, MNRAS 286, 23
 Baker J.C., Hunstead R.W. 1995, ApJ 452, L95
 Barkana R. 1997, ApJ 489, 21
 Casali M., Hawarden T. 1992, JCMT-UKIRT Newsletter No.4, 33
 Coleman G.D., Wu C.-C., Weedman D.W. 1980, ApJS 43, 393
 Courbin F., Magain P., Keeton C.R., Kochanek C.S., Vanderriest C., Jaunsen A.O., Hjorth J. 1997, A&A 324, L1
 Fioc M., Rocca-Volmerange B. 1997, A&A 326, 950
 Hodapp K.-W., Hora J.L., Hall D.N.B., Cowie L.L., Metzger M., Irwin E., Vural K., Kozlowski L.J. et al. 1996, New Astronomy 1, 177
 Impey C.D., Falco E.E., Kochanek C.S., Lehár J., McLeod B.A., Rix H.-W., Peng C.Y., Keeton C.R. 1998, ApJ 509, 551
 Keeton C.R., Kochanek C.S. 1997, ApJ 487, 42
 Keeton C.R., Kochanek C.S., Falco E.E. 1998, ApJ 509, 561
 Kozlowski L.J., Vural K., Cabelli S.C., Chen C.Y., Cooper D.E., Bostrup G.L., Stephenson D.M., McLevige W.L. et al. 1994, Proc. SPIE 2268, 353
 Kristian J., Groth E.J., Shaya E.J., Schneider D.P., Holtzman J.A., Baum W.A., Campbell B., Code A. et al. 1993, AJ 106, 1330
 Kundic T., Cohen J.G., Blandford R.D., Lubin L.M. 1997, AJ 114, 507
 Michalitsianos A.G., Oliverson R.J., Nichols J. 1996, ApJ 461, 593
 Motohara K., Maihara T., Iwamuro F., Oya S., Imanishi M., Terada H., Goto M., Iwai J. et al. 1998, Proc. SPIE 3354, 659
 Saha P., Williams L.L.R. 1997, MNRAS 292, 148
 Schechter P.L., Bailyn C.D., Barr R., Barvainis R., Becker C.M., Bernstein G.M., Blakeslee J.P., Bus S.J. et al. 1997, ApJ 475, L85
 Tonry J.L. 1998, AJ 115, 1
 Weymann R.J., Latham D., Angel J.R.P., Green R.F., Liebert J.W., Turnshek D.A., Turnshek D.E., Tyson J.A. 1980, Nature 285, 641
 Yoshii Y., Takahara F. 1988, ApJ 326, 1

Table 1. Values of elements in matrices

Band	a	b	θ
J	1.15	1.00	21
K'	1.12	1.08	33

Table 2. Photometric Results

Image	Magnitude*		Color
	J	K'	$J - K'$
A1	16.13(16.44)	15.21(15.48)	0.92
A2	16.70(17.01)	15.64(15.91)	1.06
B	18.10(18.41)	17.03(17.30)	1.07
C	17.66(17.98)	16.58(16.85)	1.08
G	17.74(18.75)	15.98(16.88)	1.76
R1	21.74 \pm 0.28 [†]	19.23 \pm 0.06 [†]	2.51
R2	21.31 \pm 0.18 [†]	19.38 \pm 0.06 [†]	1.93

* Corrected total magnitude (see text). The magnitudes inside parentheses are measured in a 0.''86 diameter aperture.

[†] Surface brightness (mag arcsec⁻²).

Fig. 1.. Full-frame image of PG 1115+080 and the reference star (star A). The small squares correspond to subarray sections in the fast readout observing mode. The object and star A were observed simultaneously.

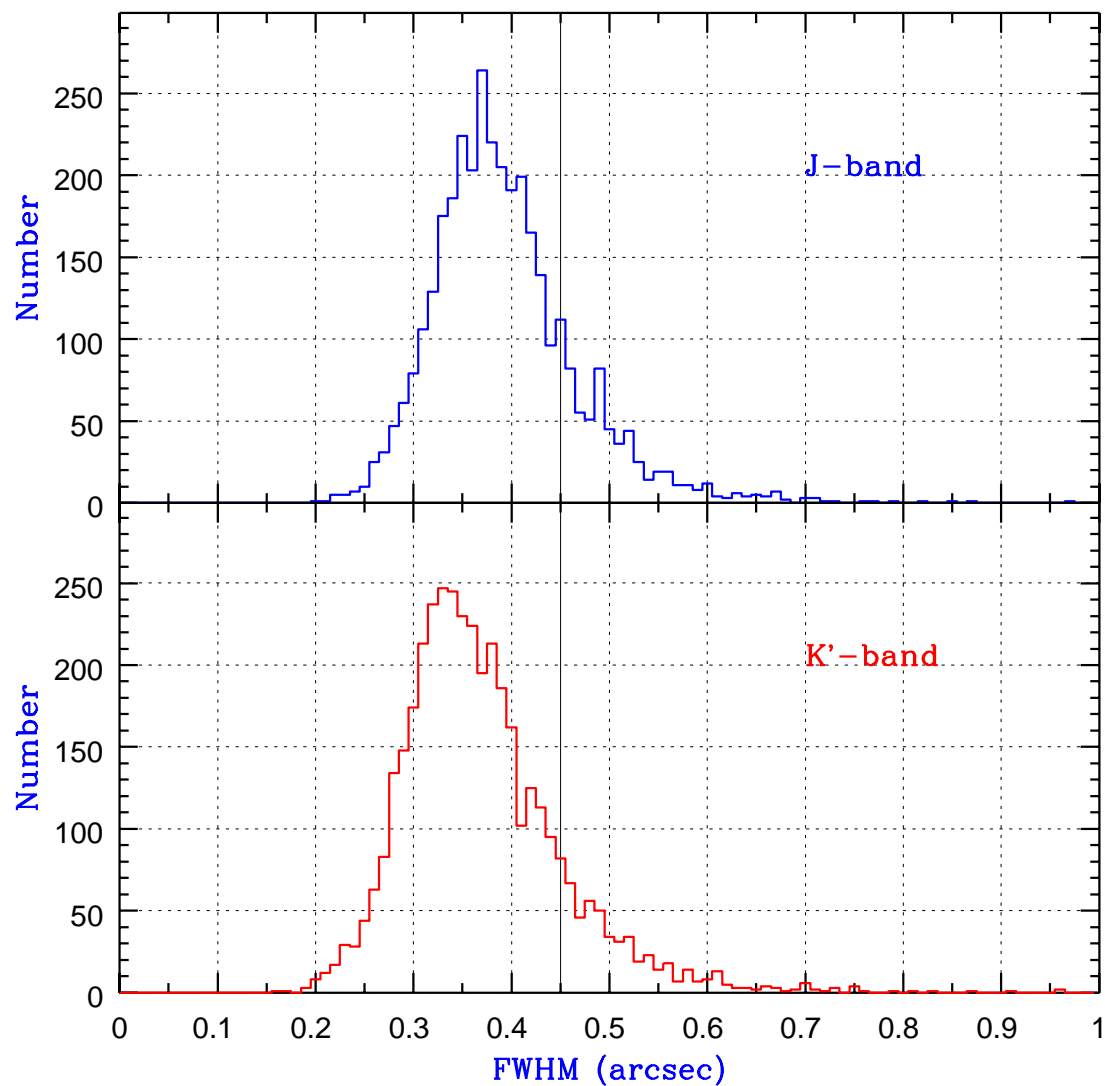


Fig. 2.. Distribution of the FWHM of star A during the observation. Only images whose FWHM was smaller than $0''.45$ were used to make the combined image.

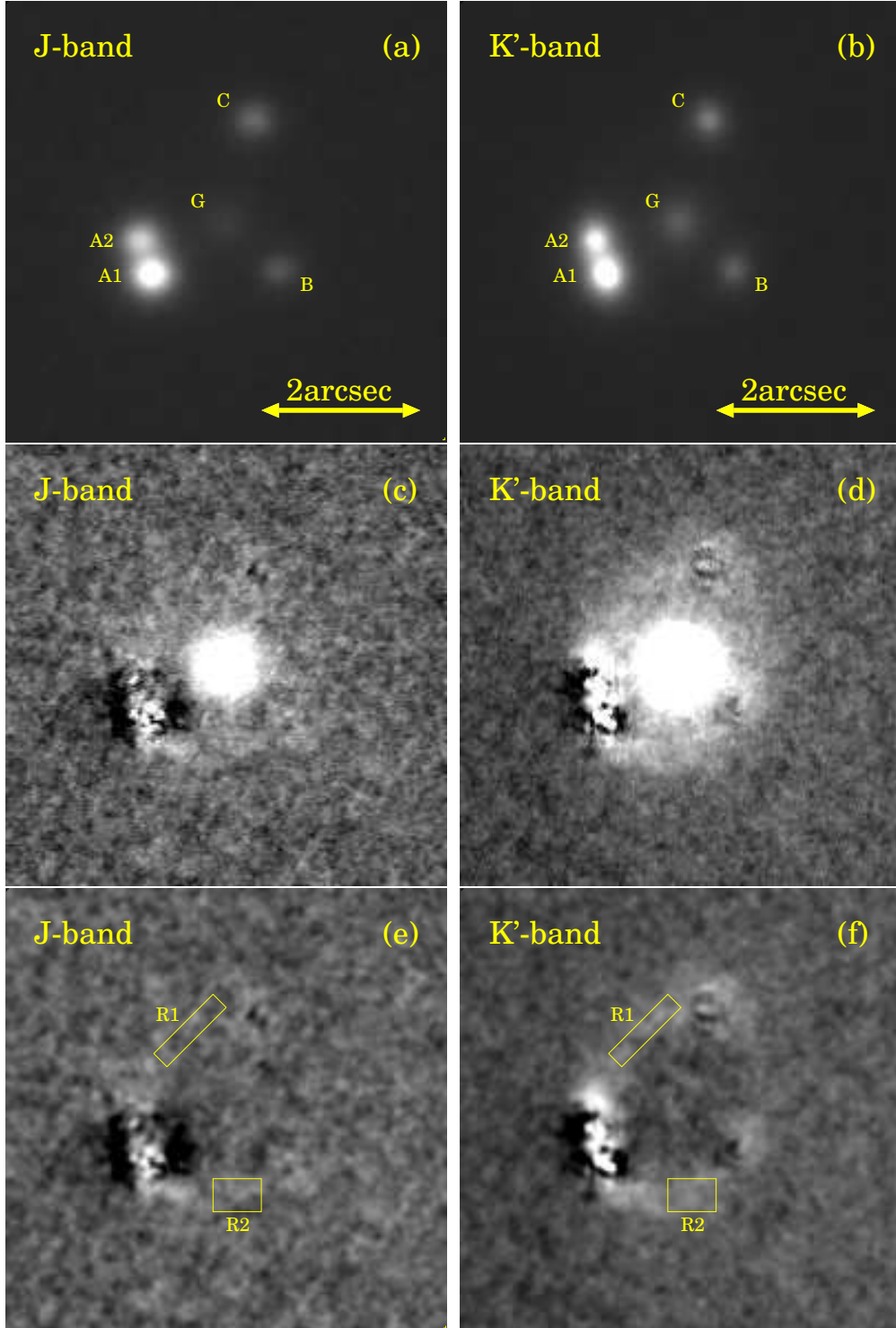


Fig. 3.. Combined images and the PSF subtraction processes. The ratio of the display range between the corresponding J and K' -band image is fixed to the flux ratio of the quasar in these bands. (a)-(b) The combined images in the J and K' -bands. (c)-(d) The image of the lensing galaxy after subtraction of the quasar component by using the transformed PSF. (e)-(f) The Einstein ring visible in the frame when the lensing galaxy image obtained by the convolved de Vaucouleurs profile (figure 4) is removed. R1 and R2 indicate the region where the surface brightness was measured.

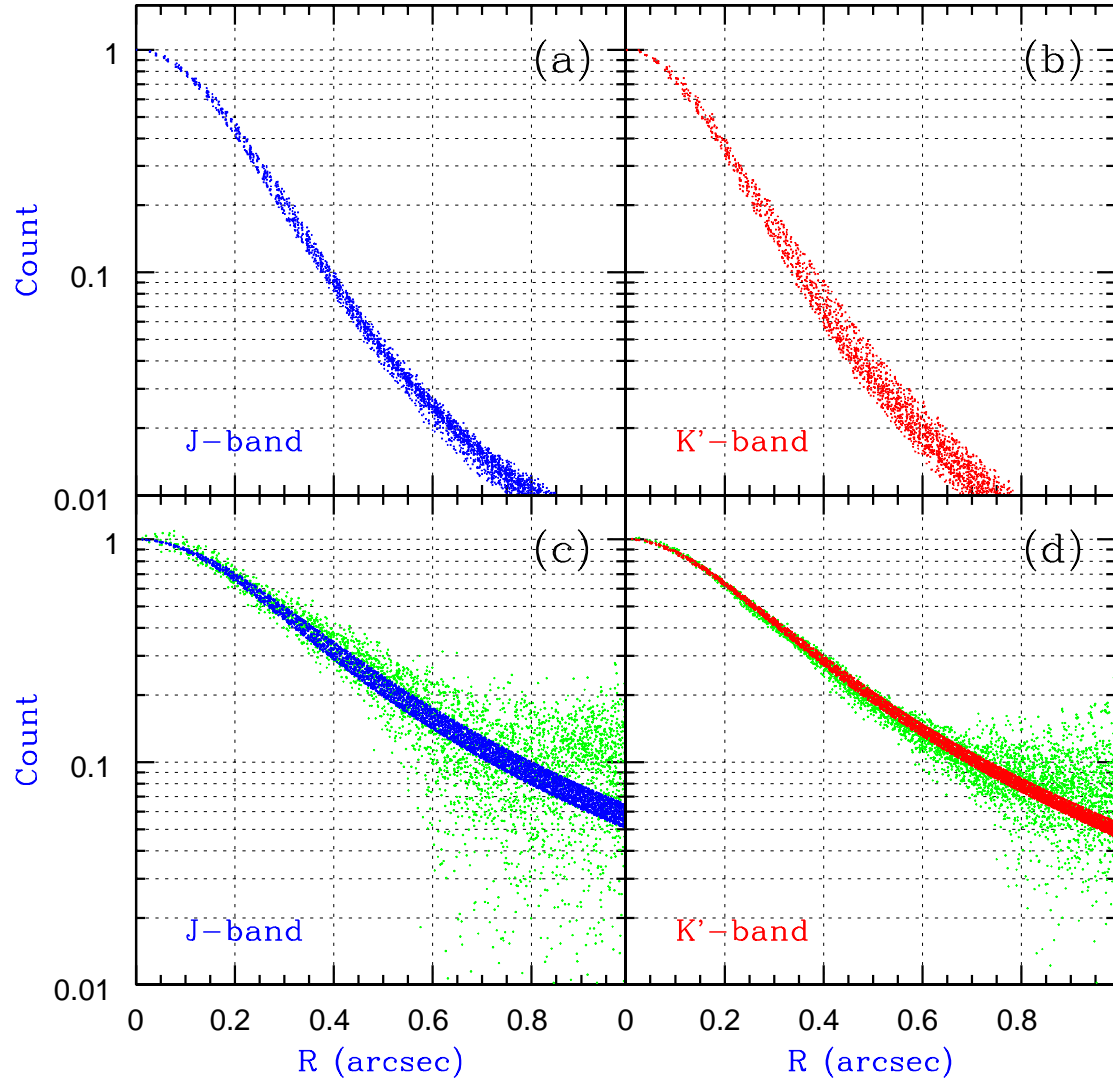


Fig. 4.. (a)-(b) Radial profile of the combined image of star A. The FWHMs are $0''.36$ (J) and $0''.32$ (K'). (c)-(d) Radial profile of the lensing galaxy and the fitted model of the PSF convolved de Vaucouleurs profile (see text).

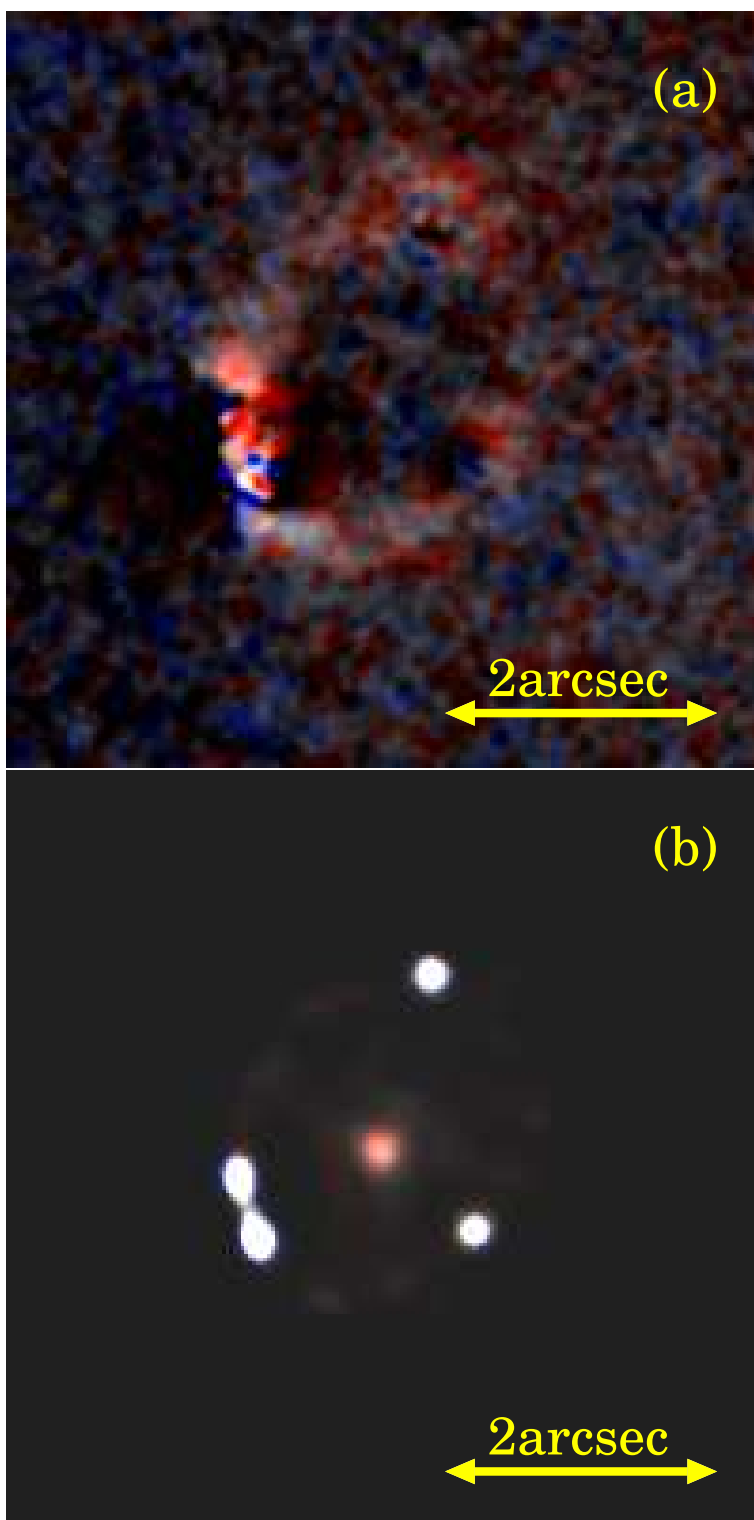


Fig. 5.. J, K' 2 color image of (a) the Einstein ring and (b) the deconvolved image (FWHM $0''.14$). Both images are displayed to make the color of component C white.

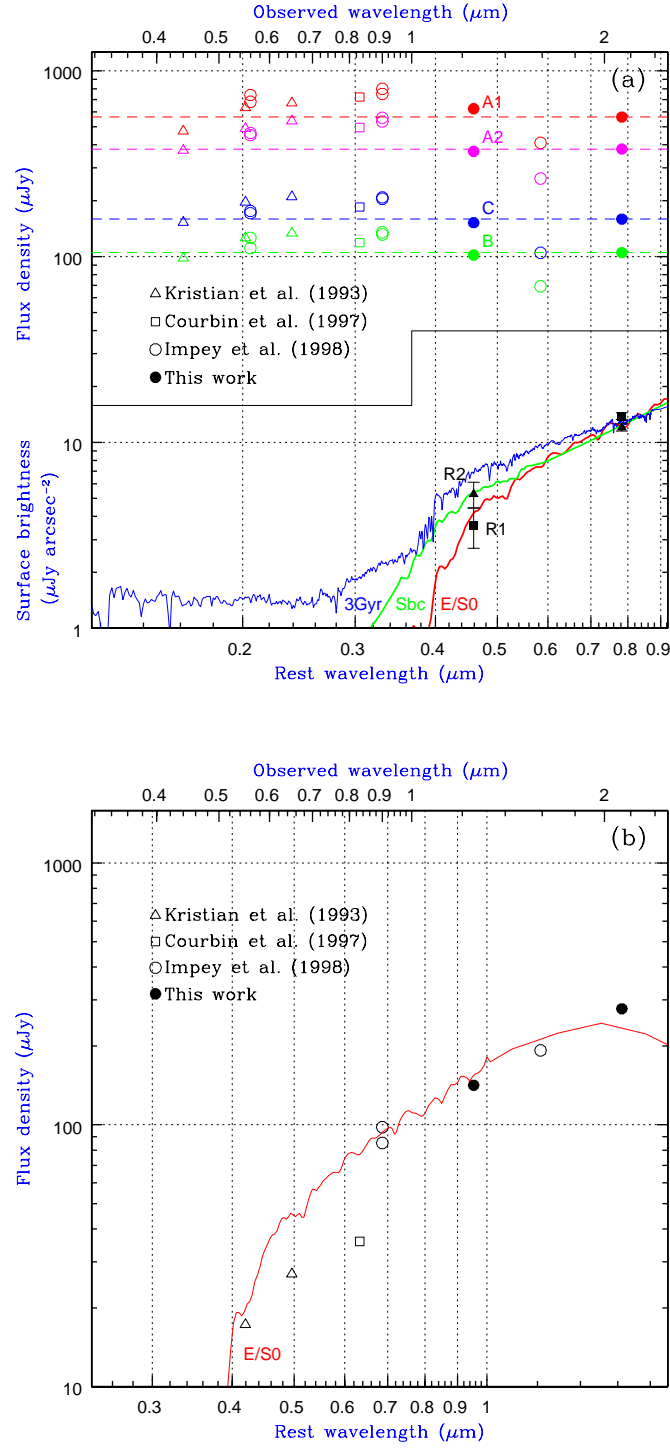


Fig. 6.. (a) SEDs of each lensed component and the Einstein ring. The thick solid lines represent the typical SEDs for E/S0 and Sbc galaxies (Coleman et al. 1980) and the thin solid line indicates the SED of the synthetic model galaxy (Fioc, Rocca-Volmerange 1997) with an age of 3 Gyr. (b) The SED of the lensing galaxy with the typical SED for E/S0 (Coleman et al. 1980; Yoshii, Takahara 1988).

This figure "fig1.gif" is available in "gif" format from:

<http://arxiv.org/ps/astro-ph/0001051v1>